Journal of Power Sources 256 (2014) 449–456

Contents lists available at ScienceDirect

Journal of Power Sources

journal homepage: www.elsevier.com/locate/jpowsour

Bulk and contact resistances of gas diffusion layers in proton exchange membrane fuel cells

Donghao Ye [a,b], Eric Gauthier [a], Jay B. Benziger [a,*], Mu Pan [b]

[a] Department of Chemical and Biological Engineering, Princeton University, Princeton, NJ 08544, USA
[b] State Key Laboratory of Advanced Technology for Materials Synthesis and Processing, Wuhan University of Technology, Wuhan 430070, China

HIGHLIGHTS

- Direct measurement of gas diffusion layer bulk and contact resistances.
- Teflon treatment increases GDL contact resistance with no change of bulk resistance.
- Microporous layer decreases contact resistance.
- Uneven compression under channels and ribs deforms GDL, breaking electrical contact.

GRAPHICAL ABSTRACT

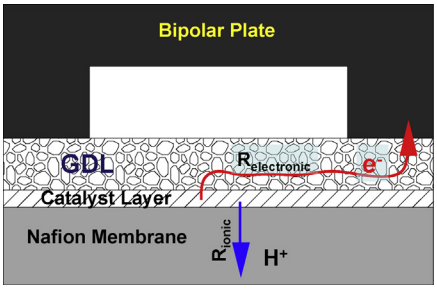

ARTICLE INFO

Article history:
Received 23 October 2013
Received in revised form
14 January 2014
Accepted 17 January 2014
Available online 24 January 2014

Keywords:
Contact resistance
Lateral resistance
Gas diffusion layer
Catalyst layer
PEMFC

ABSTRACT

A multi-electrode probe is employed to distinguish the bulk and contact resistances of the catalyst layer (CL) and the gas diffusion layer (GDL) with the bipolar plate (BPP). Resistances are compared for Vulcan carbon catalyst layers (CL), carbon paper and carbon cloth GDL materials, and GDLs with microporous layers (MPL). The Vulcan carbon catalyst layer bulk resistance is 100 times greater than the bulk resistance of carbon paper GDL (Toray TG-H-120). Carbon cloth (CCWP) has bulk and contact resistances twice those of carbon paper. Compression of the GDL decreases the GDL contact resistance, but has little effect on the bulk resistance. Treatment of the GDL with polytetrafluoroethylene (PTFE) increases the contact resistance, but has little effect on the bulk resistance. A microporous layer (MPL) added to the GDL decreases the contact resistance, but has little effect on the bulk resistance. An equivalent circuit model shows that for channels less than 1 mm wide the contact resistance is the major source of electronic resistance and is about 10% of the total ohmic resistance associated with the membrane electrode assembly.

1. Introduction

Proton exchange membrane fuel cells (PEMFCs) require both low ionic and low electronic resistivity to achieve high efficiency. Oxidation and reduction reactions take place at the membrane/catalyst layer interface. Protons are transported through the polymer electrolyte membrane and electrons are transported through the catalyst layers and the gas diffusion layer. Most research has focused on the ionic resistance of the membrane as it poses the largest potential loss. However, the potential losses for the electron current through the bipolar plate (BPP), gas diffusion layer (GDL) and catalyst layer (CL) can reduce the overall power output from a PEMFC [1,2]. In this paper we examine the factors that affect the potential losses associated with electronic current in the membrane electrode assembly (MEA).

* Corresponding author.
E-mail address: benziger@princeton.edu (J.B. Benziger).

0378-7753/$ – see front matter © 2014 Elsevier B.V. All rights reserved.
http://dx.doi.org/10.1016/j.jpowsour.2014.01.082

There have been many experimental reports and computational simulations of the fuel cell electronic resistivity. In order to minimize the electronic resistance, researchers have examined a variety of bipolar plate materials, including graphite [3–5], carbon composites [6,7], untreated and plated stainless steel [8–11] and alloys [12]. Electronic resistance is also affected by manufacturing processes including injection molding [13,14], surface treatments [15–17] and structure optimization [18–20]. Davies et al. [21] compared different bipolar plate materials and found the lowest contact resistance between the BPP and the GDL was obtained with Poco® graphite (Decatur, TX); the protective oxide on stainless steel resulted in a greater contact resistance for stainless steel BPPs. Akiki et al. [22] also compared different bipolar plate materials and found the lowest contact resistance between the BPP and the GDL was obtained with Poco® graphite. Zhang et al. [23] and Lai et al. [24] estimated the transverse contact resistance between the BPP and the GDL as a function of compression. They found the contact resistance decreased with increasing clamping pressure. Zhou et al. [25] investigated the effect of the non-uniformity of the contact pressure distribution on the electronic contact resistance. Their results showed that the electrical contact resistances was reduced by less than 30% by making the clamping pressure distribution more uniform. Ismail et al. [26] reported that the contact resistance between the GDL and the BPP increased with increasing polytetrafluoroethylene (PTFE) loading in the GDL. Miyazawa et al. [27] investigated the electrical properties of the GDL and the BPP and concluded that the contact area between the GDL and the BPP showed no noticeable increase with increasing compression pressure above a level of 0.8 MPa.

GDLs are often coated with a thin layer of carbon particles as a microporous layer (MPL) to assist in water management. Park et al. [28,29] studied the effects of PTFE content and carbon loading in the MPL on the performance of fuel cells. They reported that the MPL reduced the contact resistance between the GDL and the catalyst layer or the bipolar plate.

Experimental devices to measure GDL resistance have generally placed a piece of the GDL material between two flat steel plates. Clamping pressure is applied to assure good contact between the GDL test samples and the steel plates. The transverse resistance between the steel plates is measured. Assuming the resistance of the steel plates can be ignored the transverse resistance is equal to the GDL resistance. The transverse resistance includes contributions from both bulk resistance in the GDL and the contact resistance between the GDL and the BPP. Different models have attempted to distinguish the contributions from the bulk resistance of the GDL and the contact resistance between the GDL and the BPP.

In PEMFCs, the electronic current is carried laterally from the channel to the ribs. The compression of the GDL is not uniform. The GDL is compressed under the ribs but is not compressed under the channel. To properly assess the electronic resistance from the channel to the rib it is necessary to determine both the lateral bulk resistivity and the contact resistance.

Dhar et al. [30] introduced a pulse method for the measurement of contact resistance and bulk resistance of semiconductors samples. Cooper et al. [31] summarized and compared the electrical test methods for on-line fuel cell ohmic resistance measurement. They suggested that users of these techniques should be cognizant of differences in these methods (current interrupt, AC resistance, high frequency resistance, HFR, and electrochemical impedance spectroscopy, EIS) to properly apply and interpret the results if accurate and useful measurements of cell resistance are to be obtained. Mishra et al. [32] appear to be the first to report the effects of different gas diffusion layer materials and contact pressure on the electrical contact resistance. They presented a fractal to predict the contact resistance as a function of pressure, material properties, and surface geometry. Liu [33] introduced a four-terminal measurement technique to determine resistivity and eliminate the thermal EMFs to improve the accuracy of the measurements. Okel et al. [34] developed a 4 electrode device that clamp the GDL with a uniform clamping pressure for the simultaneous measurement of bulk and contact resistances of materials used in fuel cells. They concluded that >90% of the resistance is associated with the contact resistance between the GDL and the BPP.

In the experiments presented here, a multi-electrode probe was designed to distinguish between the contact resistance and bulk resistance through the GDL. The resistances of carbon cloth and carbon paper GDL materials are compared as functions of compression and PTFE loading. The contact and bulk resistances of catalyst layers and MPL layers have also been measured. A simple equivalent circuit model is presented to show how the resistance is reduced by the addition of a GDL in a PEMFC.

2. Experimental

Fig. 1 is a schematic of a vertical cut across a PEMFC. The principle role of the GDL is to carry the electronic current from the catalyst layer under the channel to the rib of the bipolar plate. It should accomplish this while minimizing mass transport resistances for gaseous reactant from the gas flow channel to the catalyst layer and for liquid water from the catalyst layer to the gas flow channel. There are five contributions to the resistance for the electronic current. The resistances of the bipolar plate (R_{BPP}), the GDL (R_{GDL}) and the catalyst layer (R_{cat}) are in parallel and connected by the interfacial resistances of the GDL with the bipolar plate ($R_{BPP\text{-}GDL}$) and the catalyst layer ($R_{GDL\text{-}cat}$). There are contributions from both lateral and transverse electron transport in the CL, the GDL and the BPP.

To measure contact and lateral resistances we constructed the GDL conductivity cell shown in Fig. 2. Different compression plates (or blocks) were employed to represent the channel/rib structure employed in the BPP flow fields. Block #0 is a flat plate. Blocks #1 and #2 are representative of the bipolar plates with different

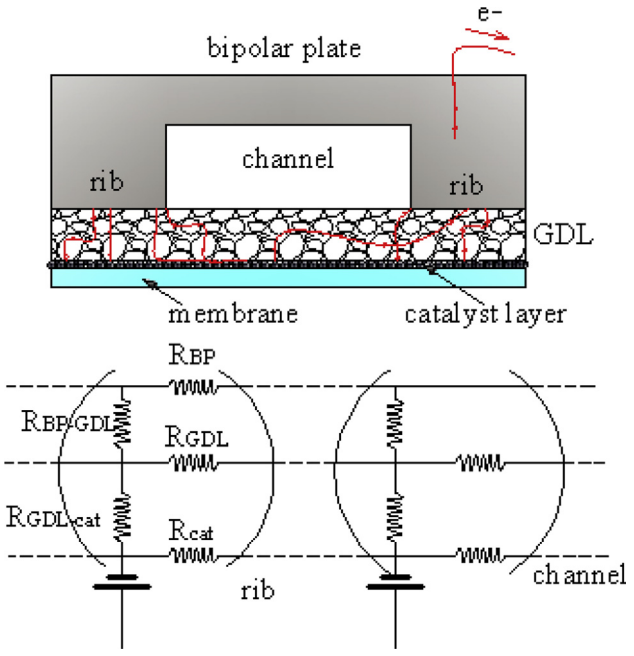

Fig. 1. Electrical resistance network model of the catalyst layer/gas diffusion layer/bipolar plate.

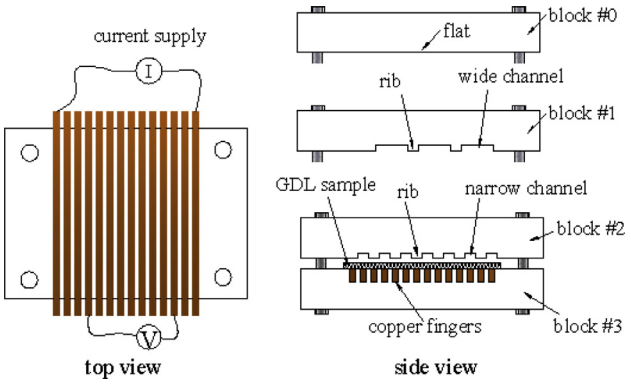

Fig. 2. Experiment schematic and installation of the GDL conductivity.

channel and rib spacing. Block #3 is the measurement block. The flow field blocks are acrylic with a series of parallel channels 1.6 mm deep separated by ribs that are 3.2 mm wide. Block#1 had 9.6 mm wide channels and Block#2 had 3.2 mm wide channels. Block #3 is a flat surface with a series of 14 parallel Cu electrodes 1.6 mm wide × 3.2 mm high × 55 mm long separated by 1.6 mm acrylic ribs. The Cu electrodes and the acrylic block were machined smooth. The Cu electrodes extended beyond the acrylic block permitting clips to be attached for electrical measurements.

The conductivity cell is operated like a 4-point conductivity probe where the distance between the inner electrodes for the voltage measurement can be varied [35,36]. The contact electrodes are made of copper in order to minimize the impact of electrode resistance.

The BPP block and the measurement block were bolted together with 4 bolts. Each of the bolts was tightened to the same torque. The clamping pressure was determined from the force applied by the four bolts divided by the area of the GDL sample being compressed.

A Hewlett–Packard (Palo Alto, CA) 6113A power supply fed a DC current of ~1–100 mA through the outermost electrodes while the voltage was measured between combinations of the inner electrodes. A precision voltmeter (BK 2831E, B&K Precision Corp., Yorba Linda, CA) measured the voltages between copper electrodes. By decoupling the current supply and voltage measurements voltage losses through the external electrical leads are eliminated. The resistance is the ratio of the measured voltage to the applied current. Resistances were measured at several different currents. To verify that the resistance measurements were not impacted by capacitive effects, AC measurements were made at frequencies from 1 Hz to 10 kHz. The AC and DC resistances were the same within experimental uncertainty.

Two commercial GDL materials were studied: carbon paper (Toray, TGP-H-120) and wet-proofed carbon cloth (CCWP). Both were obtained from the Fuel Cell Store (Fuel Cell Earth LLC, Stoneham, MA). The primary difference between these is the structural arrangement of the fibers. Carbon cloth and carbon paper are composed of 5–10 μm diameter graphitic-like carbon fibers [37,38]. Carbon paper has fibers randomly deposited and pressed into a paper sheet with a porosity of ~78% [39–41]. Carbon cloth is made by bundling fibers (approximately 100 fibers) and weaving those bundles together to form a cloth that is ~85% porous material [42].

GDL materials are frequently treated with PTFE to make them more hydrophobic. The hydrophobic treatment is thought to reduce liquid water accumulation in the GDL. The resistances of GDL materials with different PTFE loadings were measured.

The resistances of a model catalyst layer were obtained by preparing carbon coated Nafion™ 115 membranes (DuPont de Nemours, Wilmington De). Vulcan carbon black (Vulcan XC72 Cabot, Boston, MA) layers, approximately 10 μm thick, were spray coated onto Nafion™ 115 membranes. The carbon coated membrane was placed in the conductivity cell with the catalyst layer in contact with the Cu electrodes.

Microporous layers (MPL) are coated onto GDL surfaces to enhance the performance of fuel cells. In this study, the electrical conductivity of the GDL with and without an MPL was measured. The MPL is a composite layer consisting of carbon black (Vulcan XC72, Cabot, Boston, MA) mixed with PTFE as a binder. A suspension of carbon and PTFE in isopropanol was sprayed onto a GDL material using a similar process as for the catalyst layer deposition. MPL layers comprised of Vulcan carbon particles with 20 wt% PTFE were spray coated onto carbon paper and carbon cloth GDL materials. The GDL materials also had 20 wt% PTFE loading. MPL mass loadings of 0, 0.5, 1.0 and 2.0 mg cm^{-2} were applied.

3. Results

3.1. Bulk and contact resistance

For each GDL and CL sample a series of resistance measurements were obtained between different sets of Cu electrodes. Representative data, plotted as resistance as a function of distance between electrodes, are shown in Figs. 3 and 4. The data shown were obtained for a CL and GDLs with 20% PTFE loading. All measurements were done at room temperature. The bulk resistances for lateral current flow through the cross-section of the GDL or the CL may be obtained from the slopes of the resistance vs. distance lines. The *y*-intercepts of the lines are the contact resistances between the GDL or the CL with the Cu electrode.

The GDL was compressed by tightening four bolts equally with a torque wrench. GDL thickness between the bipolar plate block and measurement block was measured with a digital micrometer. Torque on the bolts was equated to an applied pressure on the GDL assuming uniform loading. GDL thickness as a function of applied pressure is summarized in Table 1.

The bulk resistivity and areal contact resistivity were determined from the slope and intercept of the resistance vs. distance line using Equations (1) and (2),

$$\rho_{\text{bulk}} = (\text{slope}) t_{\text{GDL}} L_{\text{GDL}} \quad (1)$$

$$\rho_{\text{contact}} = (\text{intercept}) w_{\text{electrode}} L_{\text{GDL}} \quad (2)$$

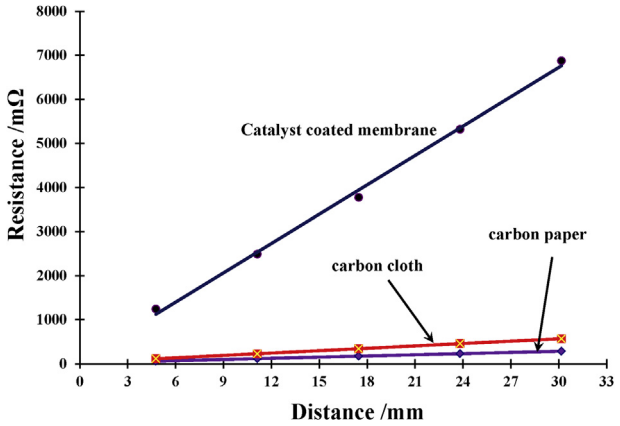

Fig. 3. Resistance as a function of electrode spacing comparing a catalyst layer (CCM), and carbon cloth and carbon paper GDL. The carbon cloth and carbon paper have 20 wt % PTFE loading. The clamping pressure was 1.08 MPa.

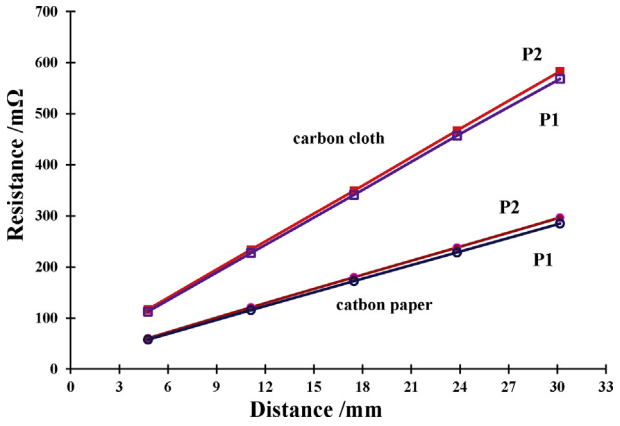

Fig. 4. Resistance as a function of electrode spacing comparing carbon cloth and carbon paper GDL. P1 and P2 represent the clamping pressures of 1.08 MPa and 0.27 MPa respectively.

where t_{GDL} is the thickness of the GDL, L_{GDL} is the length of contact between the GDL and the copper electrodes (55 mm), and $w_{electrode}$ is the width of the copper electrodes (1.6 mm).

The lateral resistance of an uncoated membrane was more than 1000 times greater than the resistance of the catalyst coated membrane. This indicated that the membrane electronic conductivity could be neglected relative to the GDL and the CL conductivity.

The total resistance of the CL is more than 100 times greater than carbon cloth and carbon paper GDL materials. The CL resistance is much greater because it is only 10 microns thick, compared to the GDLs which are ~300 microns thick. After correcting for the layer thickness the bulk resistivity of the catalyst layer is still 5–10 times greater than the bulk resistivity of the GDL materials. The carbon fibers of the GDL materials carry electronic current with much less resistance than the resistance encountered with multiple point contacts between carbon particles in the CL. Table 2 is a comparison summary of the bulk resistivity and areal contact resistivity of the CL, carbon cloth GDL and carbon paper GDL.

The areal contact resistivity of the CL with the Cu electrode is approximately 2–4 times greater than the area contact resistivity of the GDL materials. The CL only makes point contacts with the electrode, while the GDL materials allow line contacts with the electrode. The line contacts provide more contact area resulting in reduced contact resistivity.

Fig. 4 shows that both the contact and bulk resistivities of carbon cloth GDLs are greater than those for carbon paper GDLs. Fig. 4 shows that neither the bulk nor the contact resistivities changed much for applied pressures from 0.27 to 1.08 MPa.

Table 1
Compression of carbon cloth and carbon paper GDL materials.

Pressure (MPa)	Thickness (t_{GDL}, μm) ±10 μm	
	Carbon paper initial thickness: 370	Carbon cloth initial thickness: 397
Initial compression	301	320
0.27	281	298
0.38	267	267
0.54	261	247
0.8	256	241
1.08	248	234
1.6	239	220
2.16	229	211

Table 2
Resistivities of catalyst layer and GDL materials.

Material	ρ_{bulk} (mΩ cm)	$\rho_{contact}$ (mΩ cm^2)
Catalyst layer	90	50
Carbon cloth GDL	10	25
Carbon paper GDL	6	13

3.2. The effects of PTFE loading on the resistivity of GDL materials

The bulk and contact resistances of carbon paper and carbon cloth GDL materials with different PTFE loadings were measured, and the results are compared in Fig. 5. The bulk resistivities for both carbon paper and carbon cloth showed no dependence on the PTFE loading. This is reasonable since the PTFE is external to the carbon fibers that carry the electronic current. The PTFE apparently filled in the voids of the GDL materials, and therefore had no effect on the network structure of the carbon fibers that carry the current.

The contact resistivities of both carbon cloth and carbon paper GDL materials increased with increasing PTFE loading, and the effect was greater for the carbon cloth. Since the PTFE coats the carbon fibers the contact of the carbon fibers at the surface of the GDL will form an insulating layer between the carbon fibers of the GDL and the Cu electrode. The greater the PTFE loading the thicker the insulating layer. Why the PTFE creates greater contact resistance with carbon cloth than carbon paper is not known, but it is suspected it is related to the larger scale morphology with the carbon cloth. The woven pattern of carbon cloth results in fewer point contacts between the GDL and the electrode material, so blocking those contact points has a greater effect on the carbon cloth.

3.3. The effects of microporous layer on the resistivity of the GDL

The microporous layer (MPL) plays a key role in improving the performance of fuel cells [43–46]. Numerous papers focus on how the MPL affects water transport to improve fuel cell performance. The MPL also alters the electronic conduction by filling in the voids of the GDL with a conducting materials and providing more points of contact at the GDL/BPP interface.

MPL layers comprised of Vulcan carbon particles with 20 wt% PTFE were spray coated onto GDL materials; mass loadings of 0, 0.5, 1.0 and 2.0 mg cm^{-2} were applied. The GDL materials also had 20 wt% PTFE loading. The bulk and areal contact resistivities of the GDL with MPL layers measured under 0.80 MPa compression are summarized in Table 3.

The addition of an MPL had no effect on the bulk resistivity of the carbon paper GDL. The addition of an MPL layer reduced the bulk resistivity of the carbon cloth GDL slightly. The addition of the MPL reduced the contact resistance for both carbon paper and carbon cloth GDL materials.

The carbon particles for the MPL appeared to penetrate into the larger depressions of the bundle weave of carbon cloth which resulted in the decrease of the bulk resistivity of carbon cloth. Since the particles did not effectively enter the carbon paper GDL there was little effect on the bulk resistivity. As shown in Table 3, the presence of an MPL slightly reduced the bulk resistivity and contact resistance. But there was little to no effect of increasing the carbon loading above 0.5 mg cm^{-2} on the bulk or contact resistance. Both carbon paper and carbon cloth GDL materials showed reduced contact resistance due to an MPL suggesting that the small particles of the MPL layer produced more contact point between the GDL/MPL layer and the Cu electrode. However, for thicker layers of carbon black there is no increase in the points of contact to the BPP. The carbon black was mixed with PTFE, increasing carbon loadings

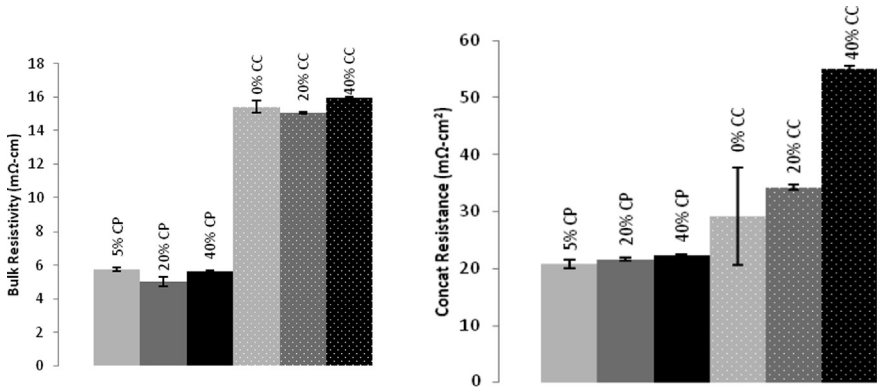

Fig. 5. Bulk resistivity and contact resistance of GDL materials (Toray Carbon Paper and Carbon Cloth) at 1.07 MPa.

also increases the PTFE content. The increased PTFE loading may limit the contact between the carbon particles and BPP.

3.4. GDL deformation and contact resistance

Increasing the torque on the bolts increased the clamping pressure on the GDL. In a fuel cell, the bipolar plate only contacts the GDL under the ribs; no pressure is applied to the GDL under the channel. To examine the effect of non-uniform pressure loading on the GDL, ribs and channels were machined into the bipolar plate blocks. The ribs and channels were spaced such that the Cu electrodes were either under a rib or a channel. Block#1 with wide channels had three electrodes under each channel and one electrode under each rib. Block#2 had one electrode under each channel and rib. By choosing pairs of electrodes it was possible to measure resistances between electrodes under the ribs or under the channels.

Fig. 6 shows the effective conductivity of carbon cloth GDL material measured between electrode 1 (under a rib) and the other electrodes for Block#1 with the wide channels. Electrodes 3 and 7 are centered under the channels. Fig. 7 shows the data for a carbon paper GDL. When the carbon paper GDL is put under sufficient compression the conductivity went to zero at electrodes 3 and 7, indicating that the GDL pulled away from the electrode at the center of the channel. As the compression was increased the carbon cloth pulled away from electrodes 2 and 4 at the edges of the channel. The carbon paper GDL required greater compression for detachment to occur, and the detachment was only seen at electrodes 3 and 7 at the very center of the channel.

The detachment of the GDL from contacting the electrode under the channel can be seen in the photo images shown in Fig. 8. The carbon cloth GDL shows a much greater deflection than the carbon paper GDL.

Table 3
Resistivities of carbon paper and carbon cloth as function of the carbon black content in the MPL.

Carbon loading in MPL	Bulk resistance (mΩ cm)	Contact resistance (mΩ cm^2)
Carbon paper		
No MPL	6.2	12.8
0.5 mg cm^{-2}	5.8	10.8
1 mg cm^{-2}	5.9	10.4
2 mg cm^{-2}	6	11.4
Carbon cloth		
No MPL	14.3	28.3
0.5 mg cm^{-2}	12.1	22.4
1 mg cm^{-2}	11.3	23.7
2 mg cm^{-2}	11	23.6

(Fig. 8) Experiments were also done with narrow channels. Block#2 had ribs and channels both 3.2 mm wide. With Block#2 the carbon cloth GDL required compression to 1.08 MPa before detachment was observed, and no detachment was observed for carbon paper GDL for pressures up to 1.61 MPa.

4. Discussion

It is frequently forgotten that the primary reason for a GDL in the PEMFC is to reduce the electronic resistance to carry the electronic current from the catalyst layer under the channel to the bipolar plate. The electrical resistance associated with the MEA is almost always much less than the resistance for ion transport in the polymer membrane. Fuel cell improvements have emphasized identification of membranes with reduced ion resistance. But there is a finite electronic resistance associated with the GDL and CL that should not be completely ignored.

The measurement method presented here clearly differentiated the contact resistance between the GDL or the CL with the BPP from the bulk resistance to carry the current laterally in the GDL. The key results from this study are:

1. The catalyst layer has a much larger resistance for electronic transport than the gas diffusion layer.
2. The addition of PTFE to the GDL increases the contact resistance, but has little effect on the bulk resistance.
3. The addition of a MPL to the GDL reduces the contact resistance. The addition of an MPL produced a small decrease in bulk

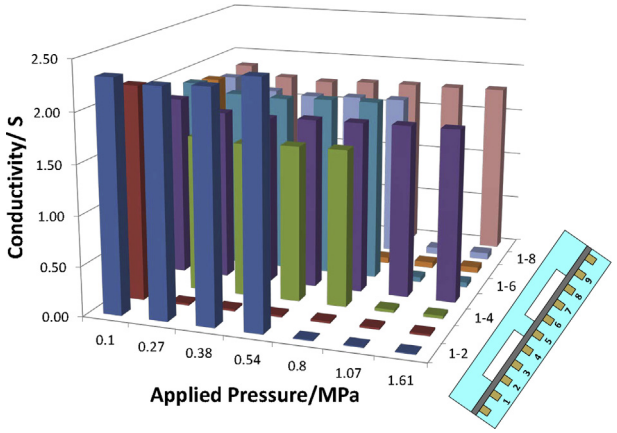

Fig. 6. Effective conductivity of carbon cloth GDL under ribs and channels as a function of the applied pressure.

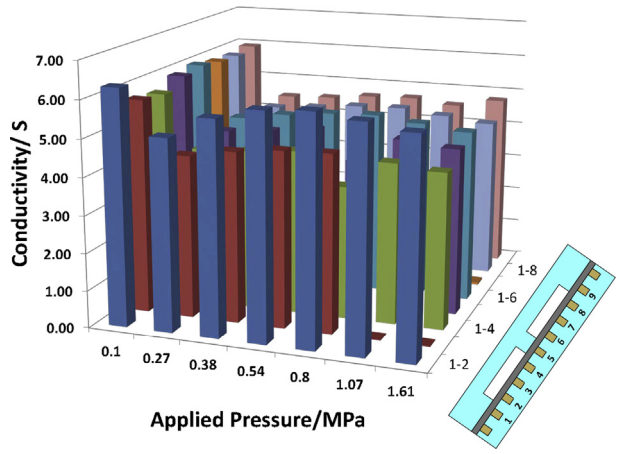

Fig. 7. Effective conductivity of carbon paper GDL under ribs and channels as a function of the applied pressure.

resistance for carbon cloth GDL, but had no effect on the bulk resistance for carbon paper GDL.

4. Compression has little effect on the bulk resistance of the GDL. Compression can deform the GDL which can cause detachment under the channel.

The results indicate that bulk resistance is not significantly altered by processing of the GDL. The GDL is made up of carbon fibers. The electron current is carried through those carbon fibers. Adding PTFE, adding an MPL or compressing the GDL has little effect on the carbon fibers, so there is little effect on the bulk resistivity. However, those treatments all affect the interface of the GDL with the bipolar plate, altering the contact resistance as was seen in the results presented above.

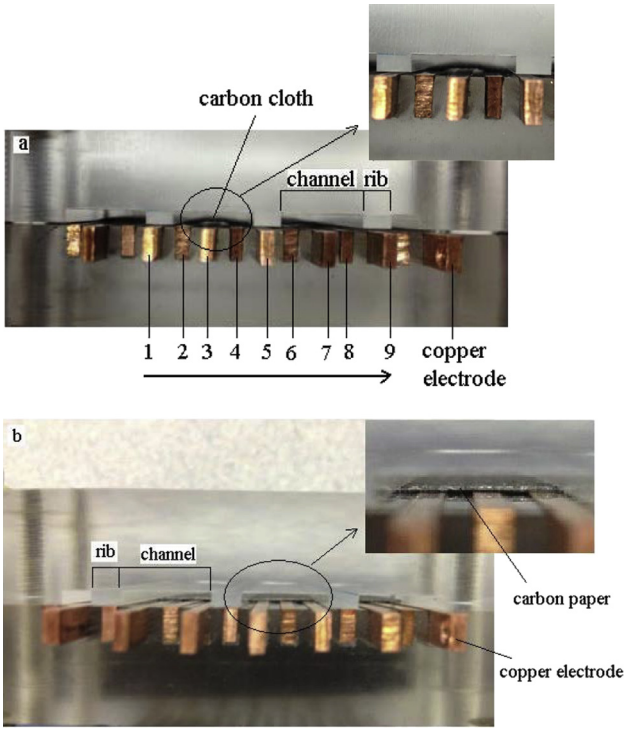

Fig. 8. Images of the GDL deflection under a channel for (a) carbon cloth and (b) carbon paper. These are at an applied pressure of 1.61 MPa.

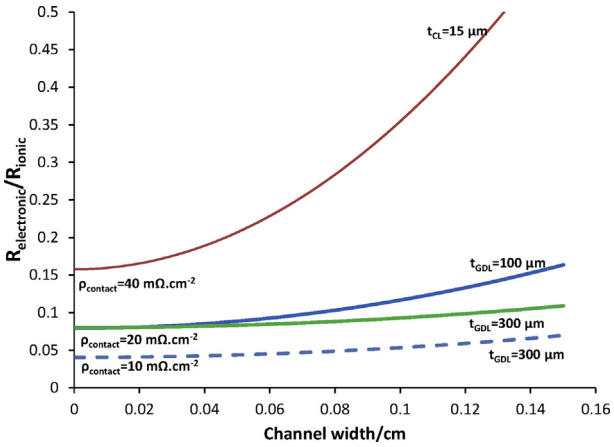

Fig. 9. ($R_{electronic}/R_{ionic}$) as a function of channel width and GDL thickness. The thickness of the conducting layer and the contact resistances are shown on the figure.

4.1. The role of the GDL on the resistivity of fuel cell

The GDL provides electrical conductivity from the catalyst layer to the bipolar plate. The catalyst layer itself is electrically conductive and could serve this role as well. However, the GDL substantially reduces the lateral resistance for electronic current conduction compared to the catalyst layer.

The effective electronic resistance of the membrane electrode assembly (MEA) is a function of the GDL thickness and the dimensions of the gas flow channel. The ohmic voltage drop in fuel cell is due to the ionic membrane resistance, the electronic resistance and load resistance. The electronic resistance involves the lateral flow of current in both the catalyst layer and the GDL from the channels to the ribs, the transverse flow of current through the catalyst layer and GDL under the ribs, and the charge transport at the GDL/bipolar plate interface, as illustrated in Fig. 1. The resistances per channel for each of those transport steps are summarized in Equation (3).

$$R_{lateral,CL} = \frac{\rho_{CL}\frac{1}{2}(w_{channel}+w_{rib})}{L_{channel}t_{CL}} \quad (a)$$

$$R_{lateral,GDL} = \frac{\rho_{GDL}\frac{1}{2}(w_{channel}+w_{rib})}{L_{channel}t_{GDL}} \quad (b)$$

$$R_{transverse,CL} = \frac{\rho_{CL}t_{CL}}{L_{channel}\frac{1}{2}(w_{channel}+w_{rib})} \quad (c) \qquad (3)$$

$$R_{transverse,GDL} = \frac{\rho_{GDL}t_{GDL}}{L_{channel}\frac{1}{2}(w_{channel}+w_{rib})} \quad (d)$$

$$R_{contact} = \frac{\rho_{contact}}{L_{channnel}\frac{1}{2}w_{rib}} \quad (e)$$

The overall electronic resistance per channel is found by adding the parallel and series resistances shown in Fig. 1. The overall electronic resistance is given by Equation (4).

$$R_{electronic} = R_{transverse,CL} + R_{transverse,GDL} + \frac{R_{lateral,CL}R_{lateral,GDL}}{R_{lateral,CL}+R_{lateral,GDL}} + R_{contact} \qquad (4)$$

We can compare the contributions of the electronic resistance to the resistance for proton transport across the membrane, given by Equation (5).

$$R_{ionic} = \frac{\rho_{ionic}t_{membrane}}{L_{channel}\frac{1}{2}(w_{channel}+w_{rib})} \qquad (5)$$

A useful figure of merit for the GDL is the ratio of the electronic resistance to the ionic resistance given by Equation (6). ($R_{electronic}$/

R_{ionic}) should be small to minimize the ohmic potential drop across the GDL.

$$\left(\frac{R_{electronic}}{R_{ionic}}\right) = \frac{\rho_{CL}t_{CL}}{\rho_{ion}t_{membrane}} + \frac{\rho_{GDL}t_{GDL}}{\rho_{ion}t_{membrane}} + \frac{\rho_{CL}\rho_{GDL}(w_{channel}+w_{rib})^2}{\rho_{ionic}(\rho_{CL}t_{GDL}t_{membrane}+\rho_{GDL}t_{CL}t_{membrane})} + \frac{\rho_{contact}w_{rib}}{\rho_{ion}t_{membrane}(w_{rib}+w_{channel})} \quad (6)$$

Under most circumstances where $\rho_{CL} \approx \rho_{GDL}$ and $t_{CL} << t_{GDL}$ the transverse resistances across the CL and GDL are negligible. The ratio of electronic to ionic resistance is dominated by the bulk lateral resistance (corresponding to the third term on the right hand side of Equation (6)) and the area contact resistance. A simplified limiting expression for the resistance ration is given by Equation (7).

$$\left(\frac{R_{electronic}}{R_{ionic}}\right) \approx \frac{\rho_{GDL}(w_{channel}+w_{rib})^2}{\rho_{ionic}t_{GDL}t_{membrane}} + \frac{\rho_{contact}}{\rho_{ionic}t_{membrane}} \quad (7)$$

In Fig. 9 the resistance ratio has been plotted as a function of the channel width (assuming the rib and channel are the same width). A Nafion™ 115 membrane with $\rho_{ionic} = 10\ \Omega$ cm was assumed. The resistivities for the GDL and CL reported in Table 2 have been used in Equation (6). The resistance ratio for just a catalyst layer with no GDL has also been shown. Lastly, we show a line corresponding to a 300 μm thick GDL with a reduced contact resistivity, which could represent the effect of a microporous layer.

Fig. 9 shows there is a minimum resistance for zero channel width. This minimum value corresponds to the contact resistance of the GDL or CL with the BPP. As the channel width increases the electronic resistance increases. With a typical GDL, 300 μm thick, there is little contribution to the electronic resistance from lateral transport for channel widths <1 mm.

There is a large reduction of the electronic resistance by introducing the GDL. The thin CL poses a large resistance for lateral transport from the channel to the rib. By placing the lower resistance GDL in parallel to the CL the effective lateral resistance for the electronic current is reduced.

Reducing the contact resistance could improve PEMFC efficiency. Resistive energy losses from the contact resistance are independent of any flow field design. From the measurements reported here those losses add ~ 8% to the resistive losses from ion transport in a Nafion™ 115 membrane. Thinner membranes can reduce the transport losses from proton transport, but will have no impact on the electronic transport. The addition of an MPL reduces the contact resistance, presumably by increasing the contact points between the bipolar plate and the GDL/MPL layer. Microporous layers are not often placed on the outer GDL surface because it hinders liquid water removal from the GDL, and flooding of the GDL may be a greater problem than the reduced electronic resistance.

In general it is expected that mass transport of gases and liquid water across the gas diffusion layer will be more important to fuel cell efficiency than the resistance for electron transport in the GDL. However, the electronic resistance should not be ignored as even small improvements in fuel cell efficiency can be important to the commercial viability of PEMFC technology.

5. Conclusion

A multi-electrode probe was employed to investigate the bulk and contact resistances of carbon paper and carbon cloth. The effects of PTFE treatment to the GDL, addition of microporous layers to the GDL, and compression of the GDL were also quantified for carbon paper and carbon cloth GDL materials.

Carbon paper has both lower bulk resistivity and contact resistivity than carbon cloth, presumably because of more uniform surface topography.

A microporous layer on carbon paper does not significantly alter the bulk resistivity of GDL materials, but does reduce the contact resistivity. The loading of carbon in the MPL can reduce the resistivity of carbon paper and carbon cloth. PTFE treatments of both carbon paper and carbon cloth GDL materials increase the contact resistivity but have little effect on the bulk resistivity of the GDL materials.

Compression of GDLs deforms the GDL under the channels and causes detachment of the GDL. Carbon cloth GDLs were more easily compressed and deformed compared to carbon paper GDLs.

The measurement of the contact and bulk resistances of GDL materials allowed quantitative analysis of the role of GDL thickness and channel width on the electronic resistance. It was shown that a GDL greatly reduced the electronic resistance for lateral electron transport compared to the resistance associated with the catalyst layer. The contact resistance was the major source of electronic resistance across GDL.

Acknowledgments

Support from the following is acknowledged by the authors: national 863 high technology item (2012AA110601) and (2013AA110201). Donghao Ye thanks CSC for financial support. Gauthier was supported by National Science Foundation Grant No. 0903661 “Nanotechnology for Clean Energy IGERT.”

References

[1] T.J. Mason, J. Millichamp, T.P. Neville, A. El-kharouf, B.G. Pollet, D.J.L. Brett, J. Power Sources 219 (2012) 52–59.
[2] C.J. Netwall, B.D. Gould, J.A. Rodgers, N.J. Nasello, K.E. Swider-Lyons, J. Power Sources 227 (2013) 137–144.
[3] P.L. Hentall, J.B. Lakeman, G.O. Mepsted, P.L. Adcock, J.M. Moore, J. Power Sources 80 (1999) 235–241.
[4] A. Hermann, T. Chaudhuri, P. Spagnol, Int. J. Hydrogen Energy 30 (2005) 1297–1302.
[5] S. Yoo, Y.H. Jang, J. Fuel Cell. Sci. Tech. 9 (2012).
[6] R.A. Antunes, M.C.L. de Oliveira, G. Ett, V. Ett, J. Power Sources 196 (2011) 2945–2961.
[7] E.A. Cho, U.S. Jeon, H.Y. Ha, S.A. Hong, I.H. Oh, J. Power Sources 125 (2004) 178–182.
[8] A. Heinzel, L. Kühnemann, T. Derieth, M. Grundler, T. Grimm, M. Kouachi, ECS Trans. 50 (2013) 25–34.
[9] J. Ihonen, F. Jaouen, G. Lindbergh, G. Sundholm, Electrochim. Acta 46 (2001) 2899–2911.
[10] S. Laedre, O.E. Kongstein, A. Oedegaard, F. Seland, H. Karoliussen, ECS Trans. 50 (2013) 829–839.
[11] J. Scholta, B. Rohland, V. Trapp, U. Focken, J. Power Sources 84 (1999) 231–234.
[12] R. Hornung, G. Kappelt, J. Power Sources 72 (1998) 20–21.
[13] F. Barbir, J. Braun, J. Neutzler, J. New. Mat. Elect. Syst. 2 (1999) 197–200.
[14] A. Heinzel, F. Mahlendorf, O. Niemzig, C. Kreuz, J. Power Sources 131 (2004) 35–40.
[15] B. Avasarala, P. Haldar, J. Power Sources 188 (2009) 225–229.
[16] Y. Show, M. Miki, T. Nakamura, Diam. Relat. Mater. 16 (2007) 1159–1161.
[17] Y. Zhou, G. Lin, A.J. Shih, S.J. Hu, J. Power Sources 163 (2007) 777–783.
[18] J.W. Lim, D.G. Lee, Compos Struct. 95 (2013) 557–563.
[19] D.H. Ye, Z.G. Zhan, J. Power Sources 231 (2013) 285–292.
[20] P. Zhou, C.W. Wu, G.J. Ma, J. Power Sources 159 (2006) 1115–1122.
[21] D.P. Davies, P.L. Adcock, M. Turpin, S.J. Rowen, J. Appl. Electrochem. 30 (2000) 101–105.
[22] T. Akiki, G. Accary, W. Charon, R. Kouta, in: IEEE 2nd International Conference on Communications, Computing and Control Applications (CCCA, 2012), 2012, pp. 1–6.
[23] L.H. Zhang, Y. Liu, H.M. Song, S.X. Wang, Y.Y. Zhou, S.J. Hu, J. Power Sources 162 (2006) 1165–1171.
[24] X.M. Lai, D.A. Liu, L.F. Peng, J. Ni, J. Power Sources 182 (2008) 153–159.
[25] P. Zhou, P. Lin, C.W. Wu, Z. Li, Int. J. Hydrogen Energy 36 (2011) 6039–6044.

[26] M.S. Ismail, D.B. Ingham, L. Ma, M. Pourkashanian, Renew. Energy 52 (2013) 40–45.
[27] A. Miyazawa, T. Himeno, A. Nishikata, J. Power Sources 220 (2012) 199–204.
[28] S. Park, J.W. Lee, B.N. Popov, J. Power Sources 163 (2006) 357–363.
[29] S. Park, J.W. Lee, B.N. Popov, J. Power Sources 177 (2008) 457–463.
[30] S. Dhar, B.R. Nag, J. Electrochem Soc. 125 (1978) 508–510.
[31] K.R. Cooper, M. Smith, J. Power Sources 160 (2006) 1088–1095.
[32] V. Mishra, F. Yang, R. Pitchumani, J. Fuel Cell. Sci. Tech. 1 (2004) 2–9.
[33] M. Liu, J. Astronaut. Metrol. Meas. 3 (2005).
[34] E. Okel, B. Schaar, O. Kanoun, in: FMTC 2008-IEEE International Instrumentation and Measurement Technology Conference, IEEE, Victoria, BC, Canada, 2008, pp. 1462–1465.
[35] V.S. Mironov, J.K. Kim, M. Park, S. Lim, W.K. Cho, Polym. Test. 26 (2007) 547–555.
[36] S. Yoshimoto, Y. Murata, K. Kubo, K. Tomita, K. Motoyoshi, T. Kimura, H. Okino, R. Hobara, I. Matsuda, S. Honda, M. Katayama, S. Hasegawa, Nano Lett. 7 (2007) 956–959.
[37] S. Chand, J. Mater. Sci. 35 (2000) 1303–1313.
[38] W.X. Zhang, J. Liu, G. Wu, Carbon 41 (2003) 2805–2812.
[39] S. Litster, G. McLean, J. Power Sources 130 (2004) 61–76.
[40] M.J. Martinez-Rodriguez, T. Cui, S. Shimpalee, S. Seraphin, B. Duong, J.W. Van Zee, J. Power Sources 207 (2012) 91–100.
[41] A. Oedegaard, C. Hebling, A. Schmitz, S. Moller-Holst, R. Tunold, J. Power Sources 127 (2004) 187–196.
[42] J.D. Larminie, A. Dicks, Fuel Cell Systems Explained, second ed., Wiley, Chichester, West Sussex, 2003.
[43] A.L. Dicks, J. Power Sources 156 (2006) 128–141.
[44] A.R. Kalidindi, R. Taspinar, S. Litster, E.C. Kumbur, Int. J. Hydrogen Energy 38 (2013) 9297–9309.
[45] J.H. Lin, W.H. Chen, Y.J. Su, T.H. Ko, Fuel 87 (2008) 2420–2424.
[46] A.Z. Weber, J. Newman, J. Electrochem Soc. 152 (2005) A677–A688.